Numerical Investigation on the Transition between Regular and Mach Reflections in Shock Waves

Numerical Investigation on the Transition between Regular and Mach Reflections in Shock Waves

Domenic D'Ambrosio and Maurizio Pandolfi

Dipartimento di Ingegneria Aeronautica e Spaziale
Politecnico di Torino
Corso Duca degli Abruzzi, 24, 10129 Torino, Italy
e-mail: domenic@athena.polito.it - pandolfi@polito.it

1 INTRODUCTION

The transition between regular and irregular shock reflections, a challenging problem in fluid dynamics, has gained practical importance in the last years because of its implications in the design of super/hypersonic air intakes.

Regular and irregular shock wave reflections were first observed and reported by Mach about 120 years ago and Von Neumann, during World War II, theoretically demonstrated the existence of a *dual solution domain*, where both configuration are potentially possible. Despite this, the problem remained open (consult the survey by Hornung [1] for a detailed bibliograpy) untill the last decade, when Li and Ben-Dor [2] theoretically demonstrated that, opposite to the contemporary belief, both the regular reflection (RR) and the irregular reflection (now frequently called *Mach reflection* (MR)) are stable in the dual-solution domain. In the same period, the hysteresis was observed experimentally for the first time [3], and a tandem numerical study [4] confirmed such results. Other experimental and numerical investigations have been reported in the last years, confirming the presence of the hysteresis, but demonstrating that the experiments are particularly sensitive to the presence of disturbances in the wind tunnel [5].

In this paper, the authors present numerical results obtained in simulating shock reflections by solving the Euler equations in two dimensions. The attention is focused on the effect exerted on the transition by the grid refinement and on the Mach stem height by the geometrical parameters that characterize the geometrical configuration. In the following section, the shock reflection problem will be shortly reminded. Then, the numerical method used will be outlined. Finally the numerical results obtained will be presented and commented.

2 REGULAR AND MACH REFLECTIONS

Two different configurations are possible when an incident shock wave is reflected on a plane surface: the *regular reflection configuration* (RR) and the *Mach reflection configuration* (MR) (figure 1). The *regular reflection configuration* is composed of two shock waves, the *incident shock* and the *reflected shock* (fig.1a).

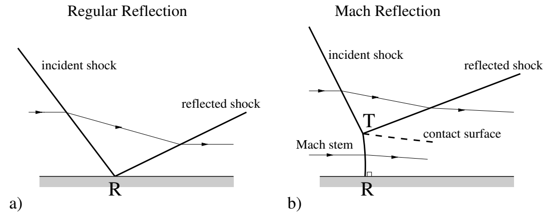

Fig. 1. Illustration of the two possible shock reflection solution: a)regular reflection and b)Mach reflection.

The flow field in the vicinity of the reflection point is divided in three parts: the undisturbed incoming flow, the region behind the incident shock and the region behind the reflected shock. In the *Mach reflection configuration*, three distinct shock waves are present: the *incident shock*, the slightly curved *Mach stem* and the *reflected shock* (fig.1b). The three shocks meet at the *triple point*, from which a *contact surface*, or *slipstream*, departs, separating the flow particles that experienced a compression through the Mach stem and those that were compressed through the incident and the reflected shocks at the same final pressure level and to the same final deflection angle, but with different entropy values. Thus, it is possible to distinguish four different flow regions in the vicinity of the triple point.

Theoretically, on the basis of the three-shocks theory developed by von Neumann, two different criteria for transition between *regular* and *Mach reflection* shock configurations can be defined. One is called the *mechanical equilibrium* or *von Neumann criterion*: it defines the minimum incident shock angle at which it is possible to obtain a MR configuration. The other is the *detachment criterion*, which defines the larger incident shock angle at which a regular reflection is still possible. In the range between the *von Neumann* incident shock angle and the *detachment* incident shock angle, both the regular and the Mach reflection are theoretically possible. The theoretical existence of a dual solution domain, demonstrated by von Neumann, implies other questions, such as the existence of an hysteresis phenomenon and the stability of the two different configurations within the domain.

Today, the existence of the hysteresis has been demonstrated both theoretically and experimentally (see, for instance [3] [4]), a theoretical study [2] has demonstrated that both the regular and the Mach reflection configurations are stable in the dual solution domain, and an analogy that provides the magnitude of the disturbance required to trigger the transition from one configuration to the other has been proposed [6].

3 NUMERICAL METHOD

In the present numerical investigation, Euler computations have been performed using a time-marching technique, a finite volume discretization over structured grids and an upwind flux-difference splitting scheme of the Osher's family [7] for the evaluation of the convective fluxes at volumes surfaces. Second order accuracy in space and in time is achieved by means of ENO-like [8] linear interpolation of Riemann invariants in the whole flow field, using a *minmod* limiter. The physical domain is divided in different zones according to a multiblock strategy.

4 NUMERICAL RESULTS

4.1 The geometrical setup

We refer to an experimental geometrical setup [3] composed of two symmetric wedges whose slope with respect to the incoming flow is varied by rotation around the trailing edge, so that the ratio between the exit cross-sectional area at the trailing edge and the wedge length is constant. The symmetrical configuration, where the reflection occurs at the symmetry axis, is necessary to avoid the shock/boundary layer interaction that would take place in experiments and in Navier-Stokes computations if the reflecting surface were a physical wall. The actual values of the geometric parameters and the free-stream conditions are chosen in order to simulate the experimental campaigns, in particular those conducted in the SH2 tunnel in Meudon, France [3] and in the T-313 and T-326 tunnels in Novosibirsk, Russia [9]. Since we will assume the flow to be inviscid, the only free-stream parameter needed is the Mach number, which is equal to 4.96. The important geometrical parameter is the ratio between the exit cross-sectional area at the trailing edge of the wedge and the wedge length, H/w. This is set equal to 0.42 when focusing on the hysteresis curve, but will be also varied to investigate the dependence of the Mach stem height from it.

The numerical geometrical setup is composed of a wedge of length w followed by a flat plate. The actual experimental configuration is different, as the flat plate is not present, but, as it will be mentioned later, such a difference does not have effect on the shock reflection. Reflecting boundary conditions are imposed at the walls and at the symmetry line, supersonic inflow and outflow conditions at the inlet and at the outlet.

Provided the Mach number is sufficiently high and if the wedge angle is in the range between the *Von Neumann angle* α^N and the *detachment angle* α^D, both the RR and the MR configurations are possible. At Mach 4.96, their theoretical values are respectively $\alpha^N = 20.87^o$ and $\alpha^D = 27.71^o$. The results obtained for a wedge angle $\alpha = 25^o$ are shown in figure 2 in terms of Mach number and pressure contours for the Mach reflection configuration only.

It is possible to recognize the *incident shock*, the *Mach stem*, the *reflected shock* and the *slipstream* (*contact surface*). The dimension of the Mach stem is controlled by the expansion fan that emanates from the trailing edge of the wedge. When the expansion fan interacts with the reflected shock, the latter is transformed in a transmitted-reflected shock, and the former in a transmitted expansion. An thick entropy layer is also generated because the transmitted/reflected shock is bended. The transmitted expansion fan reaches the slipstream and accelerates the subsonic flow behind the Mach stem until it reaches

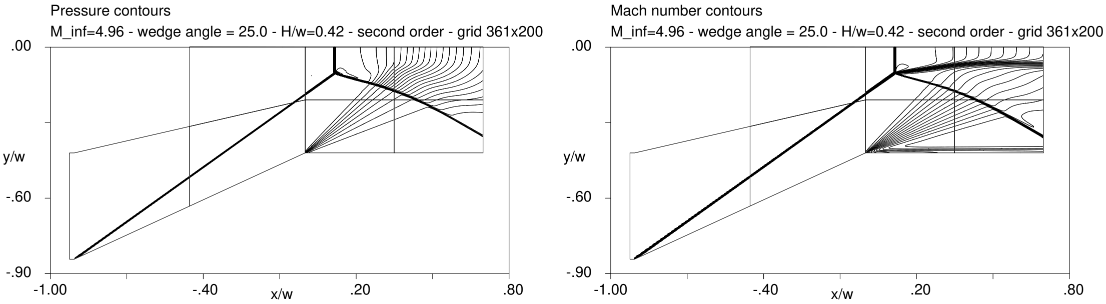

Fig. 2. Mach reflection configuration. $M_\infty = 4.96$, wedge angle $\delta = 25^o$, $H/w = 0.42$. Pressure contours (upper) and Mach number contours (lower).

sonic conditions. A convergent two-dimensional channel is thus formed between the symmetry axis and the contact surface. After the sonic point, the channel diverges and the flow continues to accelerate in supersonic conditions. Between the Mach stem and the sonic throat, limited by the symmetry axis and the slip-stream, a subsonic pocket exists in an otherwise supersonic flow. The dimensions of the subsonic pocket, and therefore the height of the Mach stem, is determined by the expansion fan, which brings the information about the geometrical configuration to the subsonic flow in the initial part of the channel. Such information, related to the ratio between the exit cross-sectional area at the trailing edge of the wedge and the wedge length H/w, propagates upstream to the Mach stem.

The presence of the flat plate behind the wedge does not have any influence on the Mach reflection, because the additional expansion waves that would emanate from the trailing edge of the wedge in case it would end abruptly, thus producing a stronger expansion, should hit the two-dimensional channel in a point where the flow is supersonic. Since the subsonic pocket is isolated from the supersonic region downstream the line composed by the sonic line at the throat and by the expansion/reflected expansion wave that hits the slipstream at the sonic point, whatever happens in such supersonic region will not affect the Mach stem.

In figure 3, the hysteresis curves obtained for Mach 4.96 and $H/w = 0.42$ using two different grids are shown. Both grids are equally spaced respectively in the direction of the symmetry axis and in the direction normal to it. The coarser grid is composed of 100 points along the wedge and 81 points along the flat plate, while 100 points discretize the domain in the direction normal to the symmetry axis. The grid refinement is doubled in the finer grid, which is composed of 200 points along the wedge, of 161 points along the flat plate and of 200 points in the normal direction. The hysteresis curves were obtained as follows. At first, computations were carried out with wedge angles ranging from values slightly lower than the *von Neumann angle* α^N to values higher than the *detachment angle* α^D. The step in the wedge angle variation was 0.5 degrees. Starting from uniform flow conditions, the configuration which results stable in the dual-solution domain was the regular reflection. When the wedge angle was sufficiently high, however, only a Mach reflection was possible. Refining the

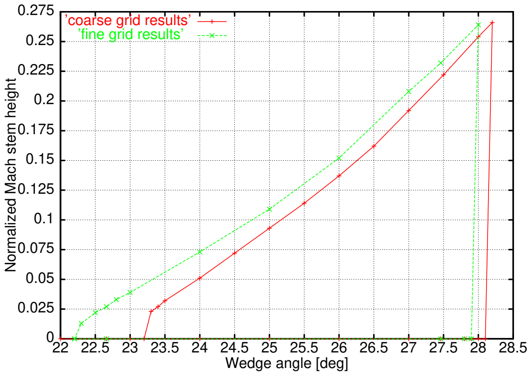

	theor.	num. fine grid	num. coarse grid
α^N	20.87^o	22.20^o - 22.30^o	23.20^o - 23.30^o
α^D	27.71^o	27.90^o - 28.00^o	28.10^o - 28.20^o

Fig. 3. Numerical hysteresis curves for Mach 4.96 and $H/w = 0.42$. The red line refers to the coarse grid (181x100), the green line to the fine grid (361x200). Theoretical and the numerical angles α^D and α^N for $M_\infty = 4.96$ and $H/w = 0.42$.

study in the wedge angle interval where the RR $\rightarrow$ MR transition occurred, the *numerical detachment angle* α^D_{num} was determined. Then, starting from a Mach reflection configuration obtained with a wedge angle higher than α^D_{num}, the wedge angle was discontinuously decreased (with a step of 0.5 degrees) and, for each step, a time integration was performed until convergence to the steady state was achieved. In this case, the Mach reflection configuration was maintained until the *numerical von Neumann angle* α^N_{num} was reached. A further decrease in the incident shock angle resulted in a smooth transition from the MR to the RR configuration. The values for the theoretical and the numerical angles α^D and α^N are given in figure 3(right).

The grid refinement study shows that the height of the Mach stem is influenced by the grid refinement. Moreover, while the RR $\rightarrow$ MR transition angle varies slightly with the grid (about 0.2^o, in figure 3), the MR $\rightarrow$ RR angle is strongly influenced by it (about 1^o), because when the two-dimensional channel becomes smaller and smaller, a very fine grid should be provided to capture it. In some preliminary experiments, not shown here, a small but not negligible influence of the limiter used in the second order on the RR $\rightarrow$ MR angle has been found. This indicates that the numerical dissipation inherent of the numerical scheme plays a certain role in determining the RR $\rightarrow$ MR transition point.

Other experiments have been conducted to determine the dependence of the Mach stem height on the H/w parameter. Maintaining the Mach number equal to 4.96 and fixing the wedge angle to 25.00^o, H/w was varied from 0.27 to 0.47, using always the same grid spacing. The related results, shown in figure 4, are in sufficiently good agreement with those obtained with the theoretical model recently proposed by Li and Ben-Dor [10] (the results shown in figure 15 of reference [10] have been extracted from the paper and are reported as line in figure 4). The effect of the ratio H/w on the fluid dynamics configuration is shown in figure 4(right) for values of H/w equal to 0.27.

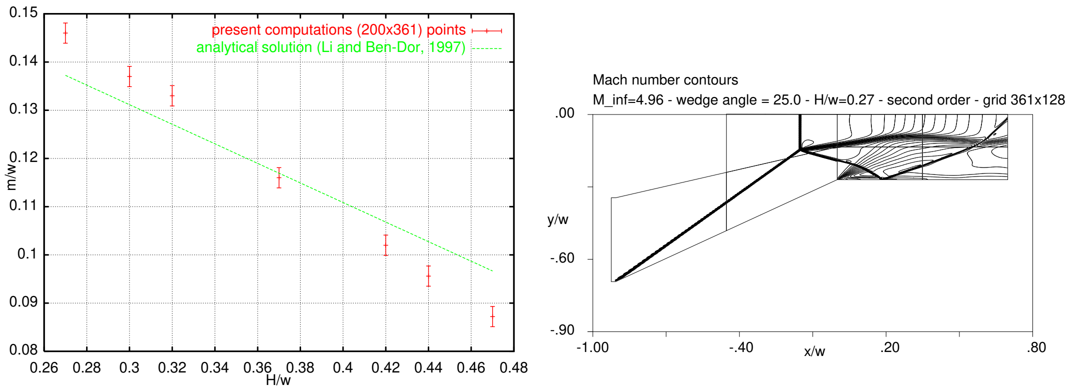

Fig. 4. Left: effect of H/w on the normalized Mach stem height m/w for Mach 4.96 and $\delta = 25^o$. Red bars: numerical results (the error bar represents the dimension of one cell in the direction normal to the symmetry axis). Green line: theoretical prediction (from figure 15 of [10]). Right: the Mach reflection configuration for $H/w = 0.27$

References

1. H.G. Hornung, "Regular and Mach Reflection of Shock Waves," *Ann. Rev. Fluid Mech.*, vol. 18, pp. 33–58, 1986.
2. H. Li and G. Ben-Dor, "Application of the principle of minimum entropy production to shock wave reflections. I. steady flows," *J. Appl. Phys.*, vol. 80, no. 4, pp. 2027–, 1996.
3. A. Chpoun, D. Passerel, H. Li, and G. Ben-Dor, "Reconsideration of oblique shock wave reflections in steady flows. part 1. experimental investigation," *J. Fluid Mech.*, vol. 301, pp. 19–35, 1995.
4. J. Vuillon, D. Zeitoun, and G. Ben-Dor, "Reconsideration of oblique shock wave reflections in steady flows. part 2. numerical investigation," *J. Fluid Mech.*, vol. 301, pp. 37–50, 1995.
5. A. Fomin, H. Hornung, M. Ivanov, A. Kharitonov, and G. Klemenkov, "The study of transition between regular and Mach reflection of shock waves in different wind tunnels," in *Proceedings of the 12st International Mach Reflection Symposium* (S. Africa, ed.), (Pilanesberg National Park), 1996.
6. N. Sudani and H. Hornung, "Stability and analogy of shock wave reflection in steady flow," *Shock Waves*, no. 8, pp. 367–374, 1998.
7. M. Pandolfi, "A contribution to the numerical prediction of unsteady flows," *AIAA Journal*, vol. 22, no. 5, 1983.
8. A. Harten, B. Engquist, S. Osher, and S. R. Chakravarthy, "Uniformly high order accurate Essentially Non-Oscillatory schemes, III," *Journal of Computational Physics*, vol. 71, 1987.
9. M. Ivanov, G. Klemenkov, A. Kudryavtsev, S. Nikiforov, A. Pavlov, A. Fomin, A. Kharitonov, D. Khotyanovsky, and H. Hornung, "Experimental and numerical study of the transition between regular and mach reflections of shock waves in steady flows," in *Proceedings of the 21st International Shock Waves Symposium* (A. Panther, Fyshwick, ed.), (Great Keppel Island, Australia), pp. 819–824, 1997.
10. H. Li and G. Ben-Dor, "A parametric study of Mach reflection in steady flows," *J. Fluid Mech.*, vol. 341, pp. 101–125, 1997.